4th International Conference on Mechanical Engineering,December 26-28, 2001, Dhaka,Bangladesh/pp. VI 239-247

A NEW THEORY AND METHODOLOGY FOR MODELING SAND PRODUCTION

A. Nouri*, M. M. Al-Darbi, H. Vaziri and M. R. Islam

Faculty of Engineering, Dalhousie University,
1360 Barrington Street, Halifax, Nova Scotia B3J 2X4, Canada.

Abstract This paper is concerned with the issue of sand production and in particular depletion induced sanding. The problem of sand production is costing the industry hundreds of millions of dollars per year. By a reliable prediction of sand production not only the sometimes unnecessary expensive sand control measures that are employed can be avoided, but also under properly designed and controlled conditions, several folds of improvement in oil and gas production can be achieved. In this paper some ideas on the physics of the problem is introduced. These ideas clarify how sanding occurs in general and more specifically under the depletion mechanism. Next, a set of unconventional triaxial tests is proposed that employ as much similar loading patterns to the real case as possible. A material model is presented for simulating the behaviour of the formation against the applied loads particularly in aged reservoirs. Furthermore, a model for numerical simulations of these experiments is presented that resembles the loading pattern on the laboratory samples. The proposed behaviour of the reservoir as a result of the depletion is numerically evaluated and covered. The result of the numerical analyses confirms the proposed model and scenario as explained. It also evaluates the effect of cohesion and friction angle and initial cap-pressure on the depletion at the time of failure. The phenomenon of the pore collapse is modelled by using a Mohr-Coulomb considering strain softening/hardening cap model.

Keywords: Modelling, sand production, depletion induced sanding.

INTRODUCTION

The relatively high depletion at the onset of sand production and low drawdown is interpreted as depletion induced formation failure mechanism. This phenomenon may subsequently lead to sand production. Classical interpretation indicates that sand production should be dominated by a shear failure mechanism in compression. Shear type failure is often observed later in the life of the reservoirs as reservoir pressures decrease and the highest stress regimen (usually overburden) transfers its load to the formation. As the reservoir depletes, the effective stress on the individual sand grains continues to increase until abandonment if pressure maintenance is not used. Therefore, if the flowing bottom-hole pressure has been significantly reduced because of reservoir depletion, and the both hydrostatic and shear stresses have become large in the reservoir, shear failure occurs both around the perforation and inside the reservoir as well (Morita et al, 1998).

All types of formations are impacted by depletion mechanism, however, depletion induced sanding is particularly pronounced in highly porous brittle rocks and formations. These formations exhibit post-peak strain-softening behaviour. Laboratory sand production experiments support the existence of depletion induced sanding in even consolidated sandstone (Veeken et al., 1991). In competent material, initial cavity failure point is little affected by fluid flow and represents a conservative stability limit in terms of the onset of sand production. In these cases, failed rock kept in place due to its internal friction appeared to prevent failure progression and show some resistance to fluid flow. But in weak material, reduction of the critical external stress with fluid flow is observed (Tronvoll et al., 1997).

In this paper, first the possible failure modes under different conditions, both physically and mechanically, are introduced. Then a constitutive law for the modelling of sand production is suggested. The proposed model will be tested by numerically simulating an experimental procedure as is introduced in this paper. The results are used to verify the ideas behind the proposed model.

NUMERICAL MODELLING OF DEPLETION INDUCED SANDING

Several analytical and numerical models are available for predicting sand production (e.g. Parkins & Wintergarden, 1998, Vaziri et al, 1997, Vaziri and Palmer, 1998, Sanffilipo et al, 1995, Morita et al, 1998,

Risnes et al, 1982, Papamichos et al, 2000). Some of these models relate sanding to the plastic strain level while others attribute it to seepage and/or erosion mechanism. In the following, we postulate the physics of sand production that would continue with a proposed constitutive relation for material behaviour modelling.

In order to distinct between the shear band formation and pore collapse mechanisms of failure, we define a critical porosity. This definition is for the sake of understanding the mechanisms and would not be quantitatively used in our analyses. This critical porosity not only depends on the physical properties of the material like grain size distributions, but also on the state of effective stresses. For the formations with porosity lower than critical, a material decementation in a limited thickness may become a predominant failure mechanism around distinct shear bands. Overall decementation generally occurs under large depletion wherein the strains (both shear and compressive) breakdown the bonding among the sand grains. Following bulk decementation, distinct sand grains can be produced by seepage forces. Whether sanding will occur depends on availability of capillary cohesion (water destroys this), strength properties of the decemented rock mass (such as projected cohesion, friction), pressure gradient (drawdown & perm), fluid velocity, fluid viscosity, perforation orientation, etc.

It should be considered that Capillary cohesion, albeit small, provides a significant resistance. Water, injected or produced, destroys the capillary cohesion, which often leads to sanding. One important point in depletion process modeling is the arch effect of the overburden. The so-called arch effect occurs because the rigidity and beam-like character of the overburden tend to limit the amount of the compaction that is transmitted to the sea or ground floor and influences the amount of compaction that occurs in the reservoir. As compaction occurs, an arch or dome of increased mean compressive stress is formed in the overburden, which causes a portion of the overburden load to be shifted from the central region of the reservoir to the flanks. These global features that result from what can be called the main "arch" are important and must be considered in the evaluation of overall compaction and subsidence phenomena (Boade et al, 1989). In the numerical analyses, considering a constant overburden pressure on the upper boundary of the model geometry leads to conservative results.

CONSTITUTIVE MODEL FOR DEPLETION INDUCED SANDING

Within the framework of plasticity theory, a mixed hardening/softening model is needed. The plastic shearing strain intensity can be a good macroscopic measure of the plastic slip, which occurs at intergranular boundaries and across microcracks. Past the state of initial yield, friction is mobilized as a function of plastic shear strain and reaches saturation at some given peak value. On the other hand, in due course of deformation, new microcracks may be activated and new ones may be formed. Therefore, it can be assumed that all deviatoric softening must be attributed to micro cracking. Possibly, the concentration of the micro-cracks would lead to material disintegration that is the necessary condition for sand production. The formation of the micro-cracks and eventually material disintegration leads to decrease of the tensile strength. This softening mechanism may be active in all stages of straining processes. However, it becomes more pronounced when the material loses its capacity to mobilize additional friction resistance. Thus, it can be assumed that during the friction-hardening phase, all tensile strength softening is negligible and it becomes noticeable only past the peak of the mobilized friction.

On the other hand, as the pore pressure in the reservoir dissipates, i.e. depletion, hydrostatic pressure as well as shear stresses increase. Therefore, permanent volume changes caused by the application of hydrostatic pressure must be taken into account. This effect is considered by including a volumetric yield surface, i.e. a cap. The hardening behaviour of the cap can be related to volumetric plastic strain. It can be assumed that volumetric plastic deformations as a result of hydrostatic pressure is activated only after the material pore collapse occurs. At the time of pore collapse, which brings about material discementation, a sudden volumetric material shrinkage occurs. A material strain hardening after the real cohesion softening is thus resulted.

In conclusion, it appears that taking Mohr-Coulomb model and keeping real cohesion constant up to the pore collapse point and then decreasing that to zero seems appealing. At the stress relaxed region near the perforations on the other hand, a bilinear Mohr-Coulomb model can be used. It is postulated that the stress relaxed region develops as the tensile failed material adjacent to the perforation is produced. In the modelling process, the strength parameters are set to zero as soon as it is tensile failed. This would indirectly simulate the erosion process that is supposed to work adjacent to the open part.

Northern Adriatic basin is a good example that clearly shows the role of material disintegration in sand production. In Northern Adriatic, a large number of gas fields experienced sand production after production start up for the most shallow wells. In deeper wells, after some years of production sanding started. The quantity of produced sand collected at the separators was always moderate but enough to cause serious operational problems. If we assume that material disintegration coincides with sand production, in ultra-weak sandstone where material pertains no cementation, sanding occurs from the beginning of the oil production. As much as the formation strength increases with depth, stress

content needed for material decementation inducement increases. Consequently, sand production is retarded with more cementation.

It is also necessary to model the post disintegration part. In this case using a cap model and also confining stress related Modulus of Elasticity for elastic part is important to be considered.
In the course of disintegration, what we know is that real cohesion finally decreases to zero. Friction angle can be considered constant. Projected cohesion can be considered to change with plastic shear strain. Real cohesion can be considered constant up to a certain shear plastic strain. Data and understanding should be improved to see if this real cohesion suddenly or gradually changes at the time of material devolution. Therefore, in this transitory stage real cohesion is changed. After disintegration happens, instead of using the linear elasticity, elasticity related to minimum effective stress would be used (elasticity parameters change). For the cemented material it seems that a linear elastic model for the first part is enough but after disintegration for the elastic part a completely different material elastic parameters considering minimum effective stress dependent elasticity needs to be considered.

ESTABLISHING A CRITERION FOR THE TIME OF PORE COLLAPSE

Very likely compaction behaviour of weak sandstone might be hypothesized as shown in Fig. 1. This Fig. depicts the reduction in porosity of the sandstone as effective stresses increase. The behaviour of sandstone, like other geomaterials, is supposed to be highly dependent to the stress history. Therefore, a preconsolidation stress hypothesis is also considered to be true in this case. At low stress levels, the sandstone deforms mainly elastically with moderate compaction per amount of applied stress. At higher stress levels, however, it begins to show larger compaction. This phenomenon of very high compressibility is referred to as pore collapse, and the sandstones compaction is divided to the two regions of elastic behaviour and pore collapse. Compaction in the pore collapse is not recovered when the stress is removed, as shown in Fig. 1.

We also suggest another hypothesis. If the material is not cemented, it could be assumed that mean pressure at the time of pore collapse is coincided with preconsolidation pressure. But, it is hypothesized that material cementation can retard pore collapse in some extent to a mean pressure above the preconsolidation pressure. Fig. 2 depicts such kind of behaviour. As shown, the material first undergoes a mainly elastic behaviour that extends up to preconsolidation point. At this point, it shows a plastic behaviour that brings about some small plastic deformation. By more increase in effective stresses as a result of reservoir depletion, material pore collapse is resulted provided that the porosity of the formation is larger than the critical porosity. The difference in preconsolidation and pore collapse pressures is assumed to mainly depend on the level of cementation of the material.

PROPOSED EXPERIMENTAL STUDY OF SAND PRODUCTION

Experimental studies play the main role in understanding both the behaviour of the material under different loading condition and also getting the required parameters for performing sand production analyses. Currently, the UCS (basically triaxial test under zero confining stress) and thick-walled cylinder test strength (TWC) are the most popular laboratory experiments. The objective of our test program is to define the mechanical behaviour of the reservoir rock under the test conditions that simulate the stress, and fluid saturation that occurs in the field. The tests must subject the rock samples to the stress levels encountered during the producing life of the field. In addition, the manner in which the stress is applied must take into account the nature of the stress environment in the reservoir. All rock in the reservoir is surrounded by adjacent rock; there are no free faces, except immediately surrounding the wellbores. So, tests to simulate sandstone in the subsurface should be confined tests that prevent the rock from undergoing any lateral deformation.

In the test, first the sample is brought to virgin in-situ conditions. The total axial stress is maintained constant. Uniaxial strain boundary conditions are established and maintained to prevent additional radial displacement. The pore pressure is reduced at a controlled rate in order to simulate depletion process. As the pore pressure is reduced, the sample will deform laterally unless the confining pressure is adjusted (reduced). The confining pressure is adjusted through the radial LVDT's which constantly measure the core's radial deformation. Signals from the LVDT's are evaluated continually by a computer, which activates a confining pressure pump when the radial deformation of the core exceeds a narrowly defined limit. Back pressure is reduced till material is failed. It is expected that at the time when pore collapse happens, a substantial deformation in the sample would be resulted.

NUMERICAL MODELING OF THE EXPERIMENTS

The studies were performed by using a computer program named FLAC, which models a continuum with a formulation derived by the finite difference technique. The formulation is explicit-in-time, using an updated Lagrangian scheme to provide the capability for large strains. A Mohr-Coulomb based cap model is used. A brief formulation of the model is presented in Appendix I.

The same loading procedure as explained for the experimental studies was used in the numerical simulations. At the beginning, the stresses and pore pressure of the sample were increased to the assumed levels of a real case. The final values of the stresses are shown in Table 1. In the process of the loading, first the confining pressure is increased to the effective mean horizontal stress level. Then, the same is increased to the total stress value, and in the meanwhile pore pressures are also increased to the assumed level of reservoir pressure. Next, the vertical stress is increased to the assumed level, while pore pressure of the sample is kept constant. From this point the main process of the loading of the sample is initiated by decreasing the pore pressure in the sample, while keeping the boundary pressures constant. This reduction continues until the sample fails. The process of pore pressure change throughout the test is depicted in Fig. 4. A sample with 7-cm diameter and 14 cm height was used in the simulations. Axial symmetric condition was assumed.

MATERIAL PARAMETERS

A whole range of different material parameters were numerically examined. The input parameters are listed in Table 1. The base parameters are friction angle of 32 degrees, cohesion of 1217 Kpa, cap-pressure of 40000 Kpa. The effect of variation of cohesion, friction angle, and initial cap-pressure on the results were studied.

PARAMETRIC STUDIES

As was mentioned earlier, the failure envelop consists of a shear envelop and a cap. The shear envelop is defined by cohesion and friction angle. The effect of the change in both of these parameters was studied in the failure pore pressure of the sample. For this purpose, at a cap-pressure of 40000 Kpa, a range of cohesion from 0 to 15000 Kpa was examined. Fig. 5 depicts the variation of the failure pore pressure with cohesion. As is seen, the collapse pore pressure is linearly related to the cohesion. Moreover, the effect although appreciable but is not tremendous. The effect of friction angle change in the failure pressure is shown in Fig. 6. Again a similar trend as found for cohesion was resulted. A linear change of the pressure with friction angle is concluded.

The effect of the parameter of the cap, the initial cap-pressure, was also studied. Fig. 7 illustrates the effect of the initial cap-pressure on the failure pore pressure. A significant effect of this parameter is seen in the results. The variation of the failure pressure seems to follow a linear pattern.

Knowing the history of the vertical displacement of the sample best helps to understand the nature of the pore collapse in the sample. A very small vertical displacement in the sample with pore pressure dissipation leading to a very sudden deformation is the pore collapse indication. On the other hand, a very gradual displacement throughout the loading process is an indication of another mechanism. Fig. 8 depicts the history of the vertical displacements with time. As seen, until a certain time, a very small deformation was resulted. This small deformation subsequently leads to a very sudden vertical deformation. In the small sample as is used in the experiments, the pore collapse most probably happens throughout the sample at once. On the other hand, in the reservoir, the pore collapse would most probably happen in the reservoir gradually, i.e. starts from one area near the wellbore and spreads throughout the reservoir gradually. Even the whole reservoir might collapse as a result of depletion.

Finally, studying the stress path of the failed elements in the sample and its relative position to the failure envelope helps in understanding the failure mode and its nature. This is illustrated in Fig. 9. As is shown in this graph, the effective stresses first meet the cap. This is the as what was predicted in the course of depletion process, as hydrostatic stress increases as a result of pore pressure dissipation. Following that, the stress path changes it's route until it meets the shear failure envelop. At this point the sample might completely fail as a result of the limited size and artificial boundaries, as it did in our case. On the other hand, in the real reservoir, compaction mode of deformation will follow the initial failure. In the meanwhile, the material gradually gains strength, mostly by increase in projected cohesion. Sand production is predicted to happen from the front open surface of the cavity and progress inward.

CONCLUSIONS

A theory for the episodic account of depletion induced sanding was introduced. Two different failure mechanisms consisting of pore collapse and formation of shear bands were introduced. Whether the pore collapse or shear band failure modes prevail depends on the porosity of the sample and the grain size distribution as well as the hydrostatic stresses at that point. Inside the reservoir, where the hydrostatic stress is high and also more increases as a result of depletion, especially in the brittle materials the pore collapse mode of failure is probably predominant. After the pore collapse occurs in the material, a post collapse compaction mechanism is replaced. By this, material starts to compact as a result of high hydrostatic stresses and as a result gets more strength with time.

On the other hand, the granulated formation material is produced from the open front surface of the cavity. A tensile progressive zone started from the initial cavity surface and developed inward the discemented material is postulated.

The hypothesized theory was numerically tested and the effect of the different material parameters was checked out on a proposed experimental strategy. Linear

correlations between the sample failure pore pressure and cohesion, friction angle and cap-pressure were worked out. The stress path of the failed elements was compared with the assumed material parameters and the consecutive modes of failure were observed.

REFERENCES

Boade, R.R., Chin, L.Y, Siemers, W.T., "Forcasting of Ekofisk Reservoir Compaction and Subsidance", *JPT* (1989).

Morita, N., Waseda, U., Burton, R.C, Eric Davis, "Fracturing, Frac Packing, and Formation Failure Control: Can Screenless Completions Prevent Sand Production?", *SPE **51187**, SPE Drilling and Completion, September* (1998).

Papamichos, E., Stavropoulou, M., "An Erosion-Mechanical Model for Sand Production Rate Prediction", *Int. J. of Rock Mech. & Min. Sci.*, **35**, 4-5 (1998).

Perkins, T.K. & Weingarten, J.S., "Stability and Failure of Spherical Cavities in Unconsolidated Sand and Weakly Consolidated Rock", *63rd Annual Conf of SPE, Houston, SPE **18244***, 613-626 (1998).

Risnes, R., Bratli, R.K., Harsrud, P., "Sand Stresses Around a Wellbore", *SPEJ*, 883-898 (1982).

Sanfilippo, F., Ripa, g., Brignoli, M. & Santarelli, F., "Economical Management of Sand Production by a Methodology Validated on an Extensive Database of Field Data", *SPE **30472**, Ann Tech Con. in Dallas* (1995).

Tronvoll, J., Skjarstein, A., Papamichos, E., "Sand Production: Mechanical Failure or Hydrodynamic Erosion?", Int. J. of Rock Mech. & Min. Sci., **34**, 3-4 (1997).

Vaziri, H., Palmer, I. & Wang, X., "Wellbore Completion Technique and Geotechnical Parameters Influencing Gas Production**",** *Canadian Geotechnical Journal*, **34**, 87-101 (1997).

Veeken, C.A.M., Davies, D.R., Kenter, C.J., Kooijman, A.P., "Sand Production Review, Developing an Integrated Approach", SPE 22792, Proc.66th Annual Technical Conference and Exhibition, Dallas, TX (1991).

Appendix I

In the model that was used, permanent volumetric deformations as a result of isotropic pressures are taken into account. This is done by using a cap model, accompanied by a Mohr-Coulomb model. Strain hardening/Softening is considered in the model. Moreover elastic parameters, shear and bulk modulus, are evolved in the course of elasto-plastic deformations. Incremental principal strains corresponding to the principal stresses are written as

$$\Delta\varepsilon_i = \Delta\varepsilon_i^e + \Delta\varepsilon_i^{pv} + \Delta\varepsilon_i^{ps} \qquad \text{(A1)}$$

Where index e stands for elastic and p for plastic and v for volumetric and s for shear deformation

Shear and volumetric failure functions, referred to as f^s and f^v, have the form

$$f^s = \sigma_1 - \sigma_3 N_\phi + 2c\sqrt{N_\phi}$$

$$f^v = 1/3(\sigma_1 + \sigma_2 + \sigma_3) + p_c \qquad \text{(A2)}$$

Where p_c is the cap pressure and

$$N_\phi = (1+\sin\phi)/(1-\sin\phi)$$

The shear and volume potential functions, referred to as g^s and g^v, corresponding to a non-associated flow rule have the form

$$g^s = \sigma_1 - \sigma_3 N_\varphi$$

$$g^v = 1/3(\sigma_1 + \sigma_2 + \sigma_3) \qquad \text{(A3)}$$

Where $N_\varphi = (1+\sin\varphi)/(1-\sin\varphi)$

Hardening parameter for shear and volumetric deformations are chosen as

$$\Delta e^{ps} = \sqrt{\frac{1}{2}(\Delta e_1^{ps} - \Delta e_m^{ps})^2 + \frac{1}{2}(\Delta e_2^{ps}) + \frac{1}{2}(\Delta e_3^{ps} - \Delta e_m^{ps})}$$

$$\Delta e_1^{pv} = \frac{1}{3}(\Delta e_1^{pv} + \Delta e_2^{pv} + \Delta e_3^{pv}) \qquad \text{(A4)}$$

Where

$$\Delta e_m^{ps} = \frac{1}{3}(\Delta e_1^{ps} + \Delta e_3^{ps})$$

Table 1: Material Parameters Used in the Numerical Simulations

Strength Parameters	Friction Angle (degree)	Cohesion (Kpa)	Cap-Pressure (Kpa)
	30-38	250-15000	35000-80000
Material Parameters	Shear Modulus (Kpa)	Bulk Modulus (Kpa)	Permeability (m^2/Pas.sec)
	206456	289789	9.87e-11
Insitu Stresses	Horizontal Stresses (Kpa)	Vertical Stresses (Kpa)	Pore Pressure (Kpa)
	93000	103000	62000

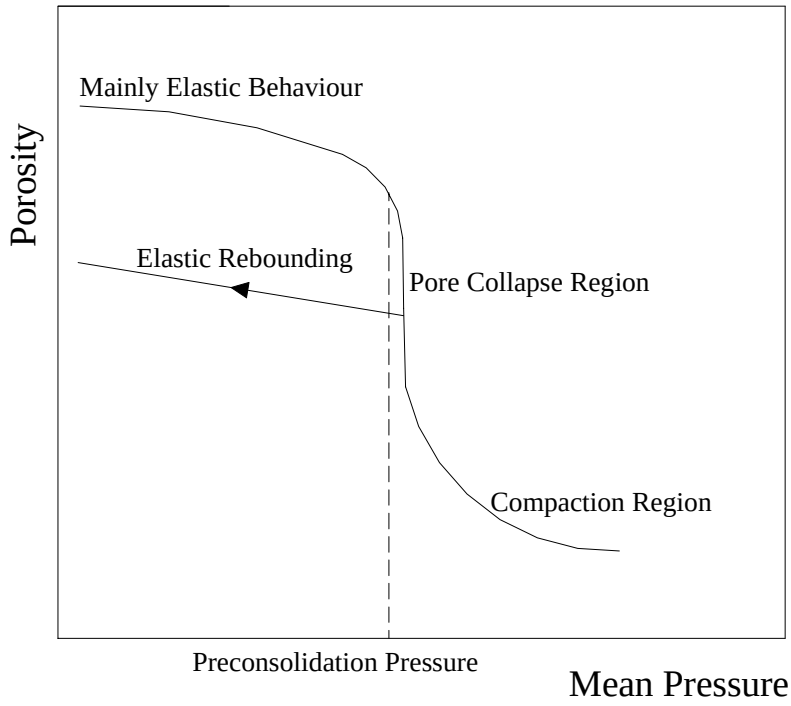

Fig. 1 Porosity/stress curve showing elastic and Pore-Collapse regions and loading and unloading paths

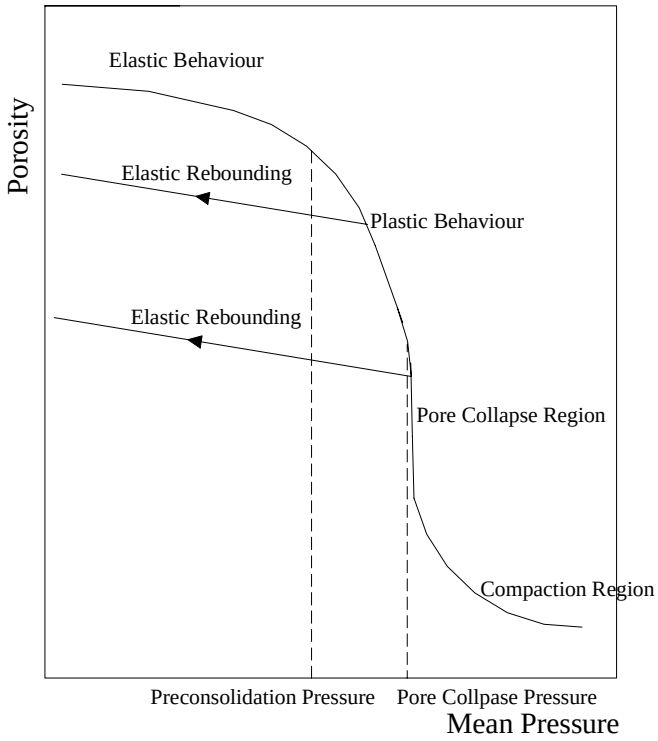

Fig. 2: Porosity/stress curve showing elastic and Pore-Collapse regions and loading and unloading paths

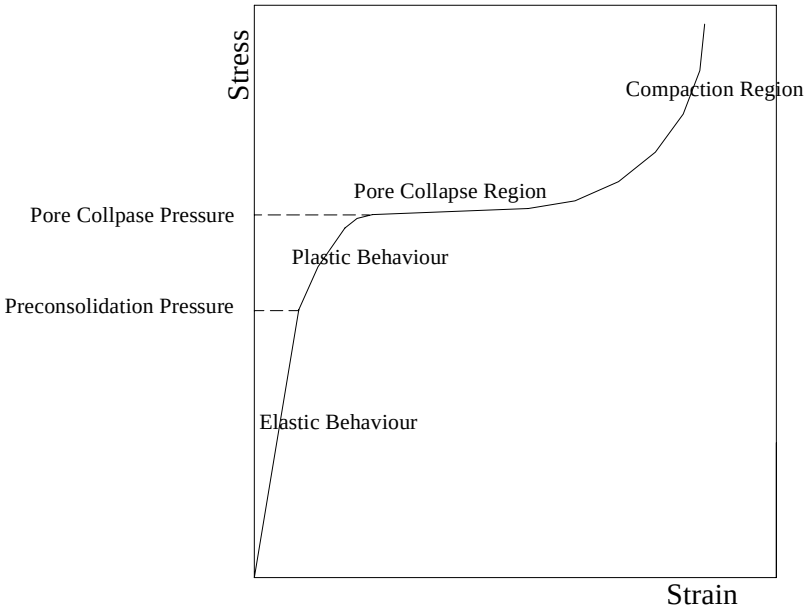

Fig. 3: General possible stress/strain behavior showing elastic, plastic and pore-collapse regions

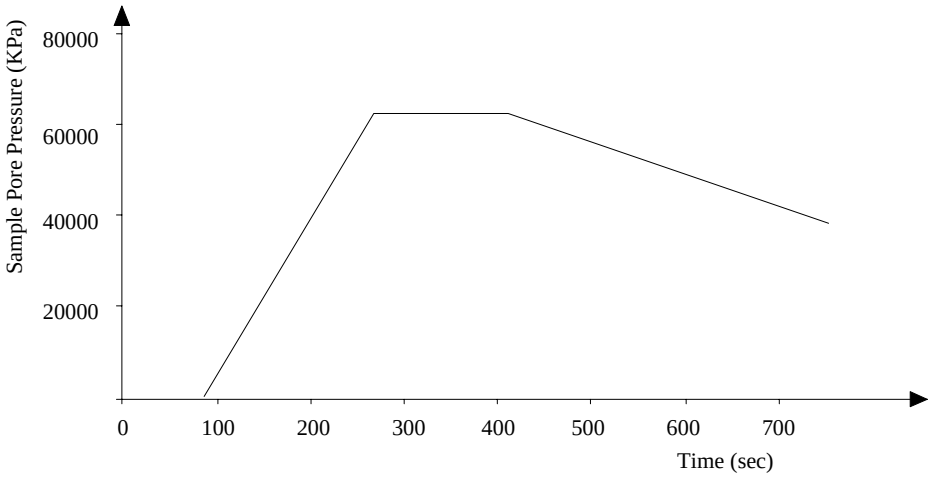

Fig. 4: Applied pore pressure in the sample

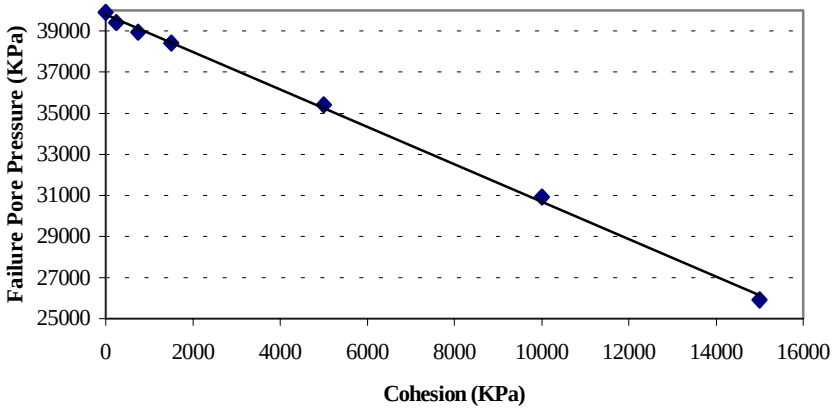

Fig. 5: Variation of failure pore pressure with cohesion

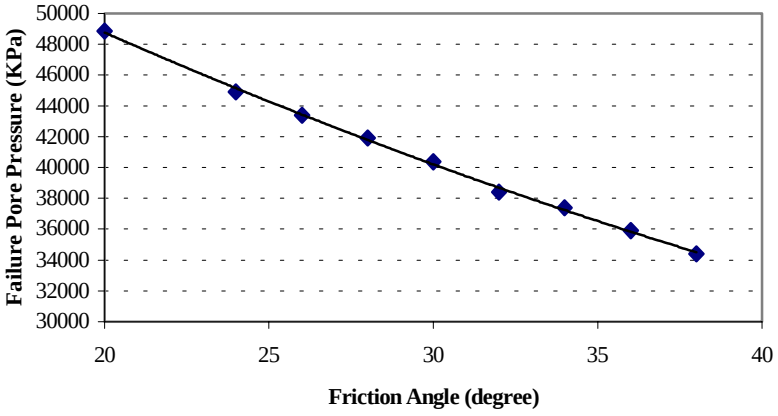

Fig. 6: Variation of failure pore pressure with friction angle

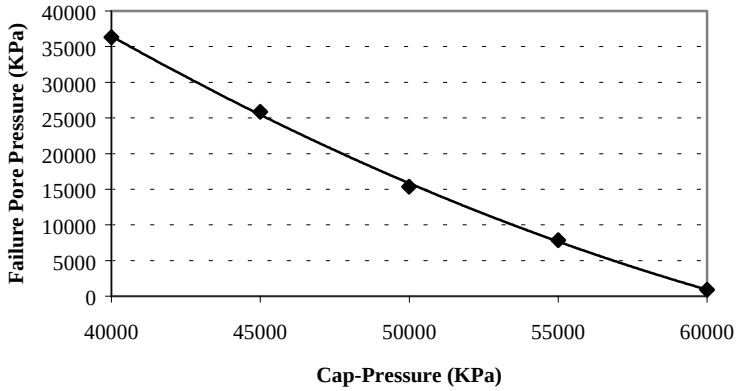

Fig. 7: Variation of failure pore pressure with initial cap-pressure

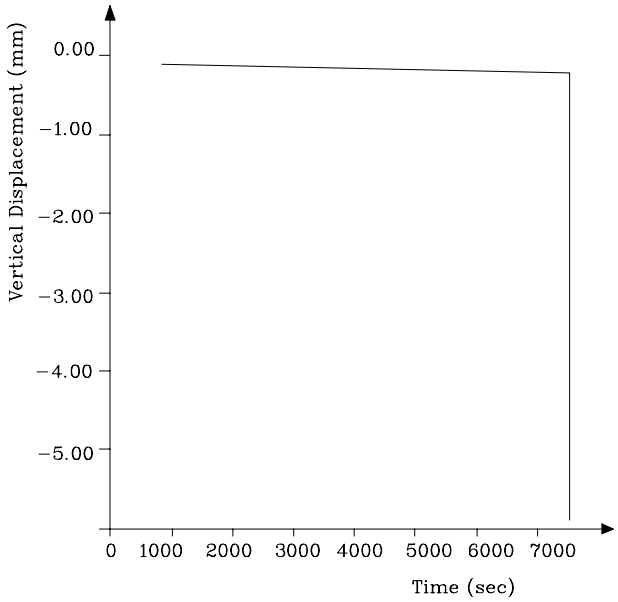

Fig. 8: The history of vertical displacements

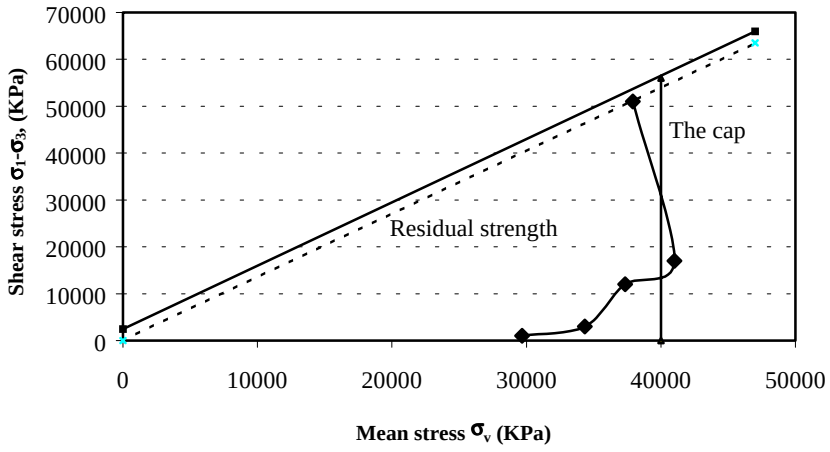

Fig. 9: Stress path of an element in the sample and it's position to failure envelope.